











ORIGINAL ARTICLE

Polycomb EZH1 regulates cell cycle/5-fluorouracil sensitivity of neuroblastoma cells in concert with MYCN

Yoshitaka Shinno^{1,2} | Hisanori Takenobu¹  | Ryuichi P. Sugino¹ | Yuki Endo¹  |
 Ryu Okada^{1,3} | Masayuki Haruta¹ | Shunpei Satoh¹ | Kyosuke Mukae¹  |
 Dilibaerguli Shaliman^{1,3}  | Tomoko Wada¹ | Jesmin Akter¹  | Kiyohiro Ando¹  |
 Atsuko Nakazawa⁴  | Hideo Yoshida² | Miki Ohira¹  | Tomoro Hishiki²  |
 Takehiko Kamijo^{1,3} 

¹Research Institute for Clinical Oncology, Saitama Cancer Center, Saitama, Japan

²Department of Pediatric Surgery, Graduate School of Medicine, Chiba University, Chiba, Japan

³Laboratory of Tumor Molecular Biology, Department of Graduate School of Science and Engineering, Saitama University, Saitama, Japan

⁴Department of Clinical Research, Saitama Children's Medical Center, Saitama, Japan

Correspondence

Takehiko Kamijo, Research Institute for Clinical Oncology, Saitama Cancer Center, 818 Komuro, Ina, Saitama 362-0806, Japan.

Email: tkamijo@saitama-pho.jp

Funding information

Saitama Cancer Center; JSPS KAKENHI, Grant/Award Number: JP19K18022; JSPS KAKENHI Grant-in-Aid for Scientific Research (B), Grant/Award Number: JP19H03625

Abstract

In the present study, we found that EZH1 depletion in MYCN-amplified neuroblastoma cells resulted in significant cell death as well as xenograft inhibition. EZH1 depletion decreased the level of H3K27me1; the interaction and protein stabilization of MYCN and EZH1 appear to play roles in epigenetic transcriptional regulation. Transcriptome analysis of EZH1-depleted cells resulted in downregulation of the cell cycle progression-related pathway. In particular, Gene Set Enrichment Analysis revealed downregulation of reactome E2F-mediated regulation of DNA replication along with key genes of this process, *TYMS*, *POLA2*, and *CCNA1*. *TYMS* and *POLA2* were transcriptionally activated by MYCN and EZH1-related epigenetic modification. Treatment with the EZH1/2 inhibitor UNC1999 also induced cell death, decreased H3K27 methylation, and reduced the levels of *TYMS* in neuroblastoma cells. Previous reports indicated neuroblastoma cells are resistant to 5-fluorouracil (5-FU) and *TYMS* (encoding thymidylate synthetase) has been considered the primary site of action for folate analogues. Intriguingly, UNC1999 treatment significantly sensitized MYCN-amplified neuroblastoma cells to 5-FU treatment, suggesting that EZH inhibition could be an effective strategy for development of a new epigenetic treatment for neuroblastoma.

KEYWORDS

5-FU, EZH1, MYCN, neuroblastoma, TYMS

Abbreviations: 5-FU, 5-fluorouracil; CCNA1, cyclin A1; ChIPseq, chromatin immunoprecipitation sequencing; EED, embryonic ectoderm development; EZH1/2, enhancer of zeste 1/2 polycomb repressive complex 2 subunit; FC, fold change; GO, Gene Ontology; GSEA, Gene Set Enrichment Analysis; H3K27me1/2/3, mono-/di-/trimethylation of lysine 27 on histone H3; MAX, MYC associated factor X; MYCN, MYCN proto-oncogene; NB, neuroblastoma; NES, normalized enrichment score; NTRK1, neurotrophic receptor tyrosine kinase 1; POLA2/DOPA2, DNA polymerase alpha 2; PRC2, polycomb repressive complex 2; qChIP, quantitative chromatin immunoprecipitation; SUZ12, SUZ12 polycomb repressive complex 2 subunit; TYMS/TS, thymidylate synthetase.

This is an open access article under the terms of the [Creative Commons Attribution-NonCommercial](https://creativecommons.org/licenses/by-nc/4.0/) License, which permits use, distribution and reproduction in any medium, provided the original work is properly cited and is not used for commercial purposes.

© 2022 The Authors. *Cancer Science* published by John Wiley & Sons Australia, Ltd on behalf of Japanese Cancer Association.

1 | INTRODUCTION

Polycomb repressive complex 2 is a multiprotein chromatin-modifying complex that is essential for vertebrate development and differentiation.¹ Polycomb repressive complex 2 is composed of a trimeric core of SUZ12, EED, and EZH1/2, which catalyzes H3K27me2/3. In many cell types, the H3K27me3 modification is associated with repression of genes encoding regulators of alternative lineages.²

The discovery of EZH1, a homolog of EZH2, confounds the previous simple interpretation of *Ezh2*-KO experiments in mice, as EZH1 associates with EED and SUZ12 to form an alternative PRC2 complex that partially compensates for the loss of EZH2 in some cell contexts.³⁻⁵ The two genes have very different patterns of expression, in that *EZH2*, but not *EZH1*, is expressed in actively dividing cells.⁴ In addition, the methyltransferase activity of EZH1-PRC complexes was shown to be very weak in comparison to that of EZH2-PRC.⁶ The EZH1-PRC2 complex appears to utilize a mechanism for compacting and repressing chromatin that is independent of its histone methyltransferase activity.⁴ Furthermore, EZH1 appears to function as a transcriptional activator in the hippocampal neurons and differentiating muscle cells.⁷⁻⁹

Recently, we analyzed the functional roles of EZH2 in NB cells and primary tumor samples using multi-omics technologies and gene-dosage regulation by lentivirus-mediated knockdown experiments. These experiments revealed that *NTRK1* (*TrkA*) is an EZH2-related epigenetic suppression target and that the depletion or inhibition of EZH2 induces the derepression of *NTRK1*.¹⁰ However, we were not able to induce effective tumor cell death in NB cells by EZH2 depletion with shRNAs or by EZH2 inhibition with the EZH2-specific histone methyltransferase inhibitor GSK126 or EPZ6438.¹⁰ These findings prompted us to further study the functional roles of the EZH2 homolog PRC2 molecule EZH1 in NB cells in the present study, with consideration of the potential development of EZH1/2 double-knockdown-related treatments of NB.

Unexpectedly, only *EZH1* depletion induced significant cell death in several NB cell lines and profoundly suppressed xenograft growth. Transcriptome and chromatin immunoprecipitation analyses of *EZH1*-depleted NB cells indicated that several cell cycle progression-related pathways were downregulated and that EZH1 plays a role as a transcriptional activator for *TYMS*, *POLA2*, and *CCNA1* in cooperation with *MYCN* in NB tumorigenesis and aggressiveness. Ultimately, these findings suggest that epigenetic therapy with an EZH1/2 inhibitor can be an important novel direction for the treatment of patients with *MYCN*-amplified NB by sensitizing the tumor cells against 5-FU.

2 | MATERIALS AND METHODS

Materials and methods are indicated in Document S1.

3 | RESULTS

3.1 | EZH proteins are highly expressed in *MYCN*-amplified NB cells

First, we evaluated the expression of PRC2-component molecules in NB cell lines. The *EZH1* mRNA expression level was not increased in the *MYCN*-amplified NB cell lines, whereas the *EZH2* mRNA level tended to increase ($p = 0.0952$; Figures 1A and S1A). The protein levels of histone methylase EZH1/2, EED, and SUZ12 were also increased in the *MYCN*-amplified NB cell lines (Figure 1B), suggesting that EZH1 accumulated at the protein level in NB cell lines. Supporting this, the *EZH2* and *MYCN* mRNA expression levels were found to be correlated positively in the SEQC-498-RPM database, whereas no positive correlation was found for the *EZH1* mRNA expression level (Figure 1C). In *MYCN*-amplified NB, high *EZH1* mRNA levels related to poorer prognosis (Figure S1B,C).

We next compared the expression of EZH1, EZH2, and H3K27me3 in eight non-*MYCN*-amplified and five *MYCN*-amplified NB tumor samples by immunohistochemistry (Figure 1D, Table S1). EZH1 was clearly expressed in the nuclei of NB tumor samples, although EZH2 signals were higher in *MYCN*-amplified NBs (EZH2: $p < 0.05$, Fisher's exact test). High H3K27me3 signals were observed in *MYCN*-amplified NBs.

3.2 | EZH1 protein accumulates by interaction with *MYCN*

To elucidate the mechanism of EZH1 accumulation, especially in *MYCN*-amplified NB cells, we induced *MYCN* expression by treatment with tetracycline in Tet-21/N cells¹¹ and detected expression of PRC2 molecules (Figure 2A). *MYCN* expression was clearly upregulated at both the mRNA and protein levels. *EZH2* was induced at the mRNA level, although *EZH1* was not. By contrast, the EZH1 protein level was strongly increased (maximum of 12-fold increase at 6 h after induction), and SUZ12/EED protein induction was also observed. As a previous report indicated a direct interaction between EZH2 and *MYCN*,^{12,13} we next undertook cotransfection of plasmids expressing these molecules to study the EZH1/*MYCN* interaction. EZH1/*MYCN* cotransfection into 293T cells resulted in both EZH1 and *MYCN* accumulation (Figure 2B), and a physical interaction between EZH1 and *MYCN* was detected (Figure 2C; MAX is a positive control *MYCN*-binding protein, and SUZ12 is a positive control EZH1-binding protein). We also confirmed that EZH1 interacts with PRC2 SUZ12 and EED in NB cells (Figure 2D). Together, these results indicate that EZH1 accumulates in *MYCN*-amplified NB cells and tumors, which might be mediated by the *MYCN*/EZH1 protein interaction.

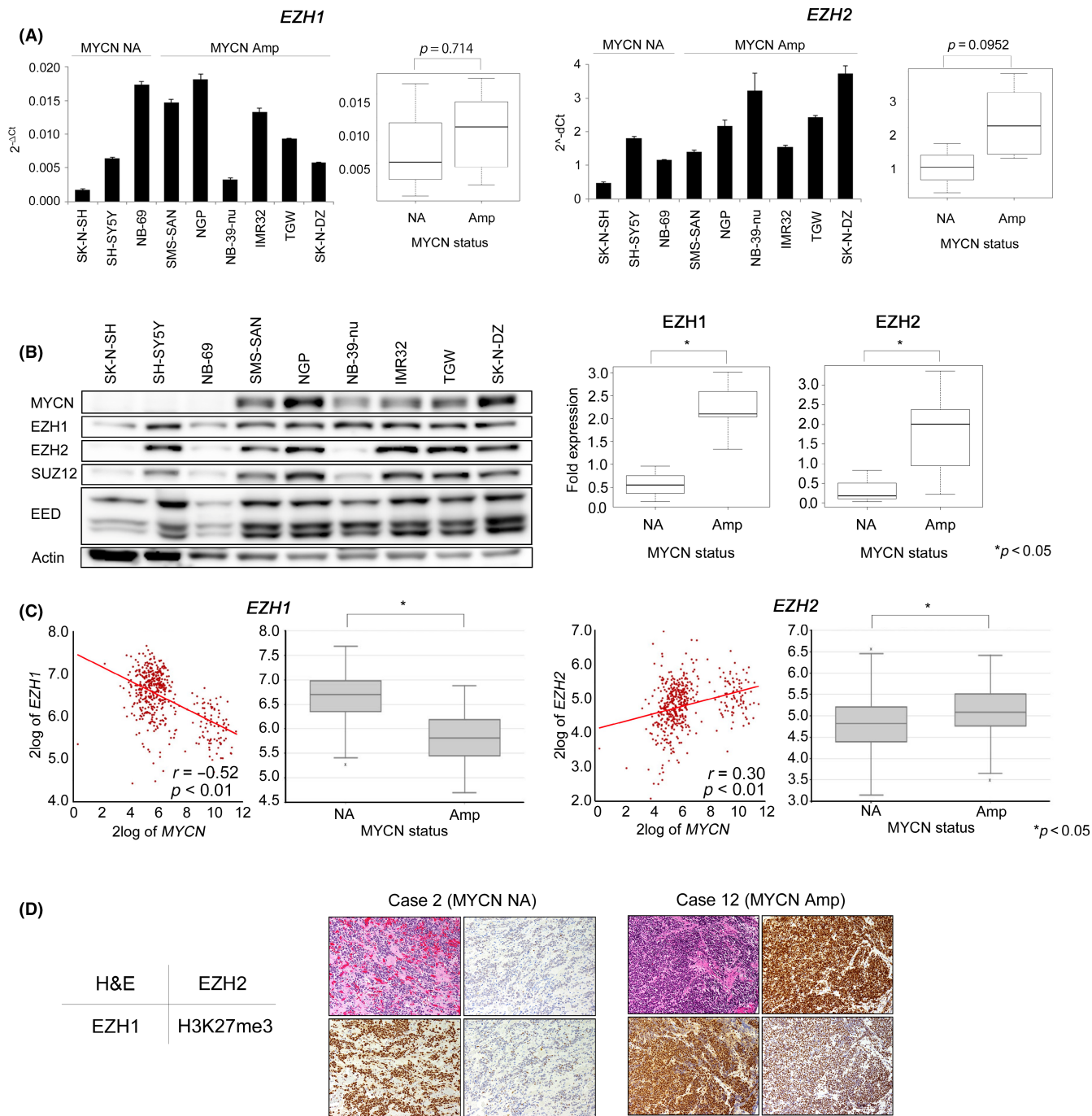


FIGURE 1 Expression profile of polycomb repressive complex 2 (PRC2) molecules in neuroblastoma (NB) cells and tumor samples. (A) *EZH1* and *EZH2* mRNA expression in NB cell lines by real-time PCR analysis. Box plot panels show the comparison of expression levels in NB cell lines with (Amp) or without (NA) *MYCN* amplification. (B) *MYCN* and PRC2 subunit protein expression in NB cell lines by western blotting. Box plot panels show the comparison of *EZH1* or *EZH2* expression in NB cell lines with or without *MYCN* amplification. $*p < 0.05$. (C) Correlation curves of *EZH1* (left) or *EZH2* (right) mRNA expression with *MYCN* mRNA in NB clinical samples from the R2 dataset. The dataset Tumor Neuroblastoma-SEQC-498-RPM-seqcnb1 was used for analysis. Box plots were studied according to the *MYCN* amplification status. (D) Representative images of immunohistochemical staining for *EZH1*, *EZH2*, and H3K27me3 of NB clinical samples Case 2 (*MYCN* NA) and Case 12 (*MYCN* Amp). All 13 case results are shown in Table S1.

3.3 | *EZH1* depletion induces apoptotic NB cell death

To study the functional role of *EZH1* in *MYCN*-amplified NB cells, we knocked down *EZH1* expression using shRNAs. We compared the efficiency of five shRNA-expressing lentiviruses for reducing the

level of *EZH1*, and ultimately selected sh*EZH1*-1¹⁴ and sh*EZH1*-2,¹⁵ which were used in previous studies (Figure S2A,B). Transfection with sh*EZH1*-1 and sh*EZH1*-2 effectively decreased the *EZH1* mRNA and protein levels (Figure 3A). Moreover, unexpectedly, *EZH1* depletion in the three *MYCN*-amplified NB cell lines resulted in significant proliferation suppression and apoptotic cell death (Figures 3B-D

and **S2C**), although depletion of the EZH1 homolog EZH2 did not induce apoptotic cell death profoundly.¹⁰ We undertook western blot analysis of p53 and caspases to study the mechanism of cell death. Although p53 phosphorylation and accumulation were not observed, caspase 7, an effector caspase, was activated in the

EZH1-depleted cells (Figure **S2D**). EZH1 knockdown also resulted in significant growth suppression accompanied by karyorrhexis in xenograft tumors (Figure **3E,F**). Taken together, these results suggest that EZH1 inhibition could be an important target for developing a new epigenetic therapy for MYCN-amplified NB.

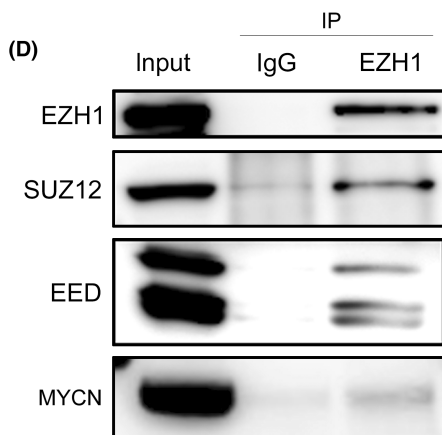
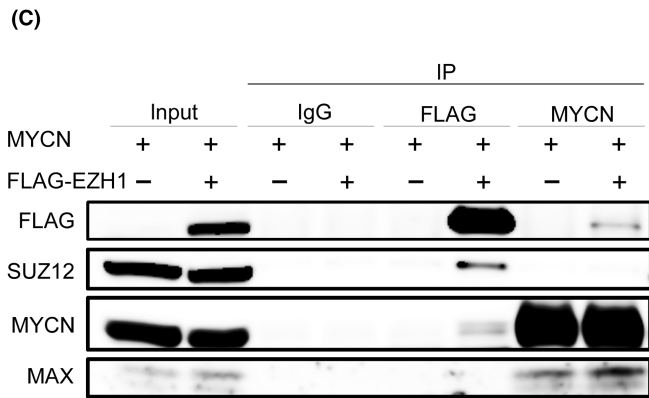
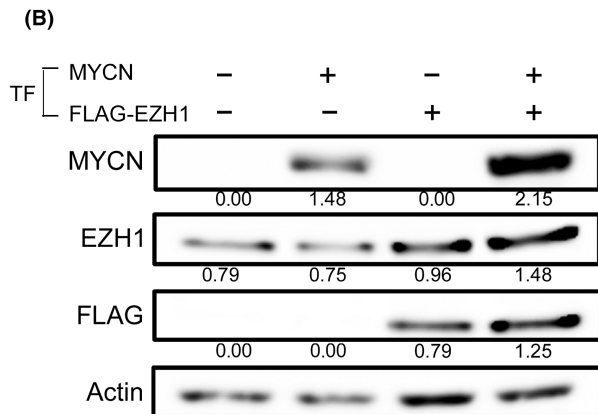
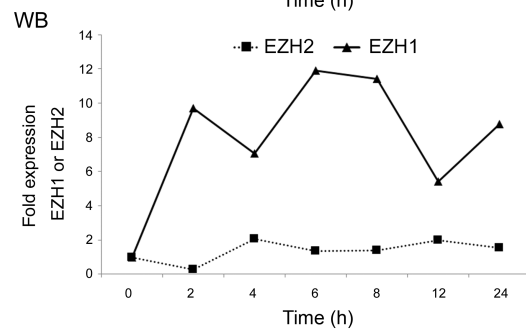
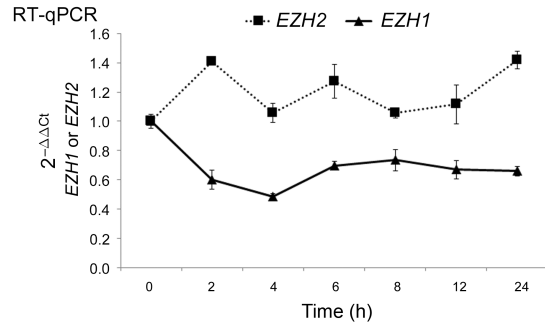
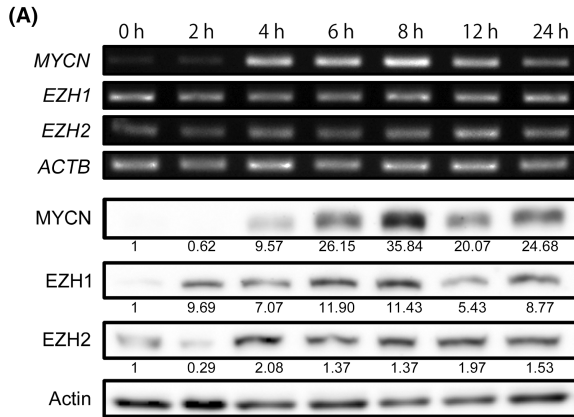


FIGURE 2 EZH1 expression correlates with MYCN in NB cells at the protein level. (A) EZH1 and EZH2 expression were studied in MYCN-inducible Tet-21/N cells. After withdrawal of tetracycline from the culture medium, cells were collected at the indicated time points and analyzed by quantitative RT-PCR (RT-qPCR) and western blotting (WB). The line graphs show EZH1 or EZH2 expression. Signal intensities were quantified by ImageJ software. Data are representative of three independent experiments. (B) Semiquantitative western blotting of MYCN and EZH1 expression in 293T cells transfected with the same amount of pcDNA3-MYCN and/or pcDNA3-FLAG-EZH1. pcDNA3-empty was used to adjust the plasmid amounts. Signal intensities were quantified by ImageJ software. (C) Immunoprecipitation (IP)-western blotting of MYCN and EZH1 expression in 293T cells. 293T cells were transfected with the same amount of pcDNA3-empty (pmock), pcDNA3-MYCN (pMYCN), and/or pcDNA3-FLAG-EZH1 (pEZH1) expression vector as indicated. After protein extraction by lysis buffer, total cell lysates were immunoprecipitated by anti-MYCN, anti-FLAG, or anti-IgG (mouse or rabbit). The MYCN-EZH1 protein complex was detected by western blotting using anti-MYCN and anti-FLAG Ab. Anti-SUZ12 and anti-MAX Abs were used for detection of PRC2 and MYCN protein complexes, respectively. (D) IP-western blotting of PRC2 complex expression in MYCN-amplified NB cells. Total cell lysates of IMR32 cells were immunoprecipitated by anti-EZH1 Ab. EZH1-PRC2 complex was detected by western blotting using anti-EZH1, anti-SUZ12, and anti-EED Ab. The binding of MYCN and EZH1 was also detected. TF, transfection.

3.4 | EZH1 depletion suppresses cell cycle progression-related pathways

To further clarify the molecular mechanism of EZH1 depletion-induced NB cell death, we carried out transcriptome analysis in the EZH1-depleted NB cell lines IMR32 and SMS-SAN (Figure S3A). First, we studied the effects of shEZH1-1 transfection in the two cell lines. A total of 346 upregulated genes and 772 downregulated genes were selected according to the criteria for differential expression (moderate *t*-test $p < 0.05$, FC > 2; see Document S1) (Figure 4A, Table S2). As EZH1 functions as a transcription suppressor or activator mediated by H3K27 methylations,^{7,8,16} depletion of EZH1 could result in both up- and downregulated expression of its target genes. Therefore, we characterized both the up- and downregulated genes using GO enrichment analysis with the DAVID tool. GO enrichment analysis of the down-regulated genes showed that several cell cycle regulation-associated pathways were highly enriched (Figure 4B). The effects of shEZH1-2 on the two cell lines are shown in Figure S3B, although only “vesicle targeting (GO:0006903)” was found to be enriched in the analysis of downregulated genes.

For further evaluation of the common pathways affected by shEZH1-1 and shEZH1-2, we undertook GSEA using the four mRNA samples extracted from the two NB cell lines transfected with shEZH1-1 or shEZH1-2. Remarkably, the E2F-mediated regulation of DNA replication pathway, which is related to cell cycle progression, was significantly downregulated in all four samples (Figures 4C,D and S3C; NES values of IMR32/sh1, IMR32/sh2, SMS-SAN/sh1, and SMS-SAN/sh2 were -1.99, -1.91, -1.83, and -2.09, respectively). A Venn diagram of the four gene groups downregulated by EZH1 depletion indicated overlap of three cell cycle-related genes: *TYMS*, *POLA2*, and *CCNA1* (Figures 4E and S3D). These genes have been reported to play important roles in cell cycle regulation and drug resistance in NB cells.¹⁷⁻²¹ We further focused on *TYMS* (protein: TS) and *POLA2* (protein: DOPA2) because Kaplan-Meier analysis using the SEQC498 data of the R2 database indicated an association between high expression of *TYMS* and *POLA2* and an unfavorable NB prognosis, but there was no such association with *CCNA1* (Figures 4F and S3E). In addition, the microarray analysis showed that expression levels of *TYMS* and *POLA2* were significantly decreased by EZH1 depletion (Figure S3F). *TYMS* (protein: TS) and *POLA2* (protein: DOPA2) transcription and protein

levels were clearly decreased in the EZH1-depleted cells (Figure 5A,B). Furthermore, TS was induced by MYCN induction in Tet-21/N cells but DPOA2 was not (Figure 5C). We next studied the effects of EZH1 knockdown on H3K27 methylation, and found that shEZH1-1 clearly suppressed H3K27me1, but not H3K27me2 or H3K27me3 (Figure 5D), suggesting the substrate specificity of EZH1.⁸ Finally, *TYMS* transcription was induced by MYCN in NB cells in luciferase analysis (Figure 5E). Together, these results indicated that *TYMS* is a MYCN target gene in NB cells, and that EZH1-related histone modification could be related to gene induction.

3.5 | EZH1 regulates MYCN binding to the *TYMS* promoter

A qChIP assay was undertaken to investigate MYCN binding to the *TYMS* promoter, which indicated that EZH1 and MYCN bind to the promoter regions in both MYCN-amplified NB cell lines (Figure 6A-C). MYCN binds to the +42 to +219 region, and MYC was previously shown to bind to the E-box sequence of this region.²² However, EZH1 binding was observed at the peripheral promoter regions and not to the +42 to +219 region (Figure 6B,C). Interestingly, EZH1 depletion by shEZH1-1 reduced the MYCN binding to the +42 to +219 region while MYCN binding to the peripheral regions increased (Figure 6D), suggesting the EZH1-related regulation of MYCN binding to chromatin.

MYCN binding, EZH1/2 binding, and important histone codes (H3K27ac, H3K4me3, and H3K27me1) were also examined by ChIP sequence assay (Figure 6E). MYCN, H3K4me3, and H3K27ac markers were found to strongly colocalize around the *TYMS* exon 1 genomic region, and EZH1 bindings were also observed from upstream of exon 1 to exon 3, suggesting the effects of EZH1 on *TYMS* transcriptional regulation in NB cells.

3.6 | EZH inhibitor UNC1999 partially mimics the effects of EZH1 depletion

UNC1999 is the first orally bioavailable inhibitor that has high in vitro potency for WT and mutant EZH2 as well as for EZH1, and is highly selective for EZH2 and EZH1 over a broad range of

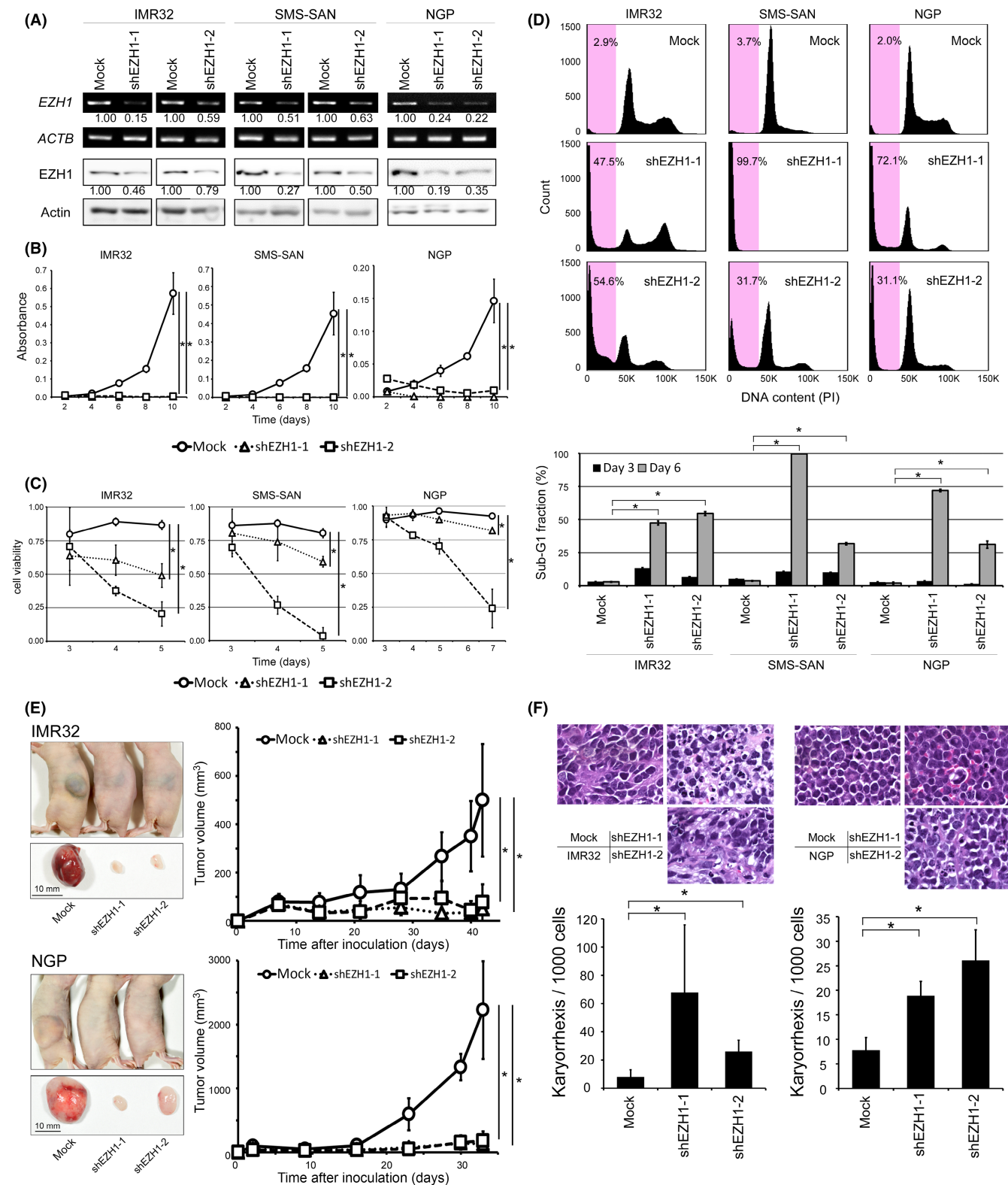


FIGURE 3 EZH1 knockdown induces apoptotic cell death in neuroblastoma cells. (A) EZH1 was knocked down by lentivirus-mediated shRNAs (shEZH1-1 or shEZH1-2) in IMR32, SMS-SAN, and NGP cells. EZH1 expression was analyzed by semiquantitative RT-PCR and western blotting. Signal intensities were quantified by ImageJ software. (B–D) WST assay (B), Trypan blue assay (C), cell cycle analysis by flow cytometry (D) of EZH1-knockdown cells. The bottom panel of (D) shows the percentage of the sub-G₁ fraction. Data are presented as the mean ± SD of at least three independent samples. **p* < 0.05. (E) Tumor development in BALB/cAJcl nu/nu mice following the injection of IMR32 and NGP cells infected with shRNA against the control (mock) or EZH1 (shEZH1-1 and shEZH1-2). Data are presented as the mean ± SD of tumors in five mice. **p* < 0.05. (F) H&E staining of xenograft tumors infected with the shRNA-expressing lentiviruses. The lower panel shows the number of cells with karyorrhexis in 1000 cells. Data are presented as the mean ± SD from three slides. **p* < 0.05.

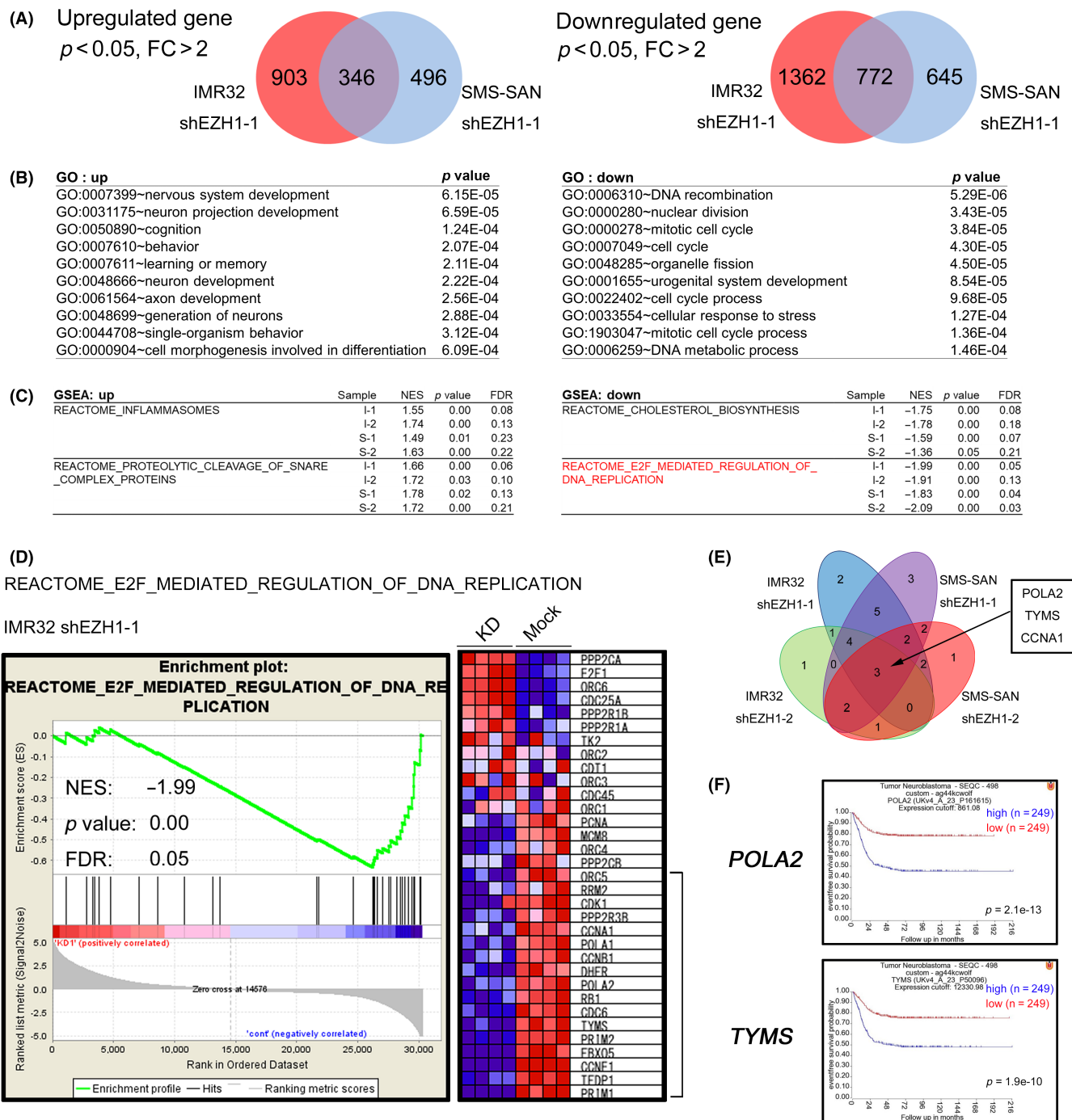


FIGURE 4 EZH1 knockdown induces cell cycle retardation and neuronal differentiation. (A–E) Transcriptome analysis was undertaken in EZH1-knocked down IMR32 and SMS-SAN cells by microarray. (A) Venn diagram of overlap among up-/downregulated genes in IMR32 and SMS-SAN cells with EZH1 knocked down by shEZH1-1. We compared the average gene expression levels between mock sample groups and EZH1-knockdown sample groups 2 days after infection. The threshold was set for p values < 0.05 in the t -test (after Benjamin-Hochberg corrections) and an absolute fold change > 2 . (B) Gene Ontology (GO) enrichment analysis for 346 upregulated genes and 772 downregulated genes indicated in (A). GO terms were limited to the biological process category. (C) Gene Set Enrichment Analysis (GSEA) was carried out in IMR32 and SMS-SAN cells with EZH1 knocked down by shEZH1-1 or shEZH1-2. The common curated gene sets of up/down enrichment in all samples are listed. I-1, IMR32 shEZH1-1; I-2, IMR32 shEZH1-2; S-1, SMS-SAN shEZH1-1; S-2, SMS-SAN shEZH1-2. (D) Details of GSEA data of REACTOME_E2F_MEDIATED_REGULATION_OF_DNA_REPLICATION in IMR32 shEZH1-1. Data are shown with the normalized enrichment score (NES), p value, and false discovery rate (FDR). In the heatmap, red represents upregulated genes and blue represents downregulated genes in knockdown samples. The right bar indicates core enrichment genes. The detail of the other samples (IMR32 shEZH1-2, SMS-SAN shEZH1-1/shEZH1-2) are shown in Figure S4C. (E) Venn diagram of overlap among core enrichment genes of the REACTOME_E2F_MEDIATED_REGULATION_OF_DNA_REPLICATION gene set in all samples. POLA2, TYMS, and CCNA1 were common downregulated genes. (F) Survival curve of clinical neuroblastoma samples according to POLA2 or TYMS expression. The dataset Tumor Neuroblastoma-SEQC-498-RPM-seqcnb1 in the R2 database was used for this analysis.

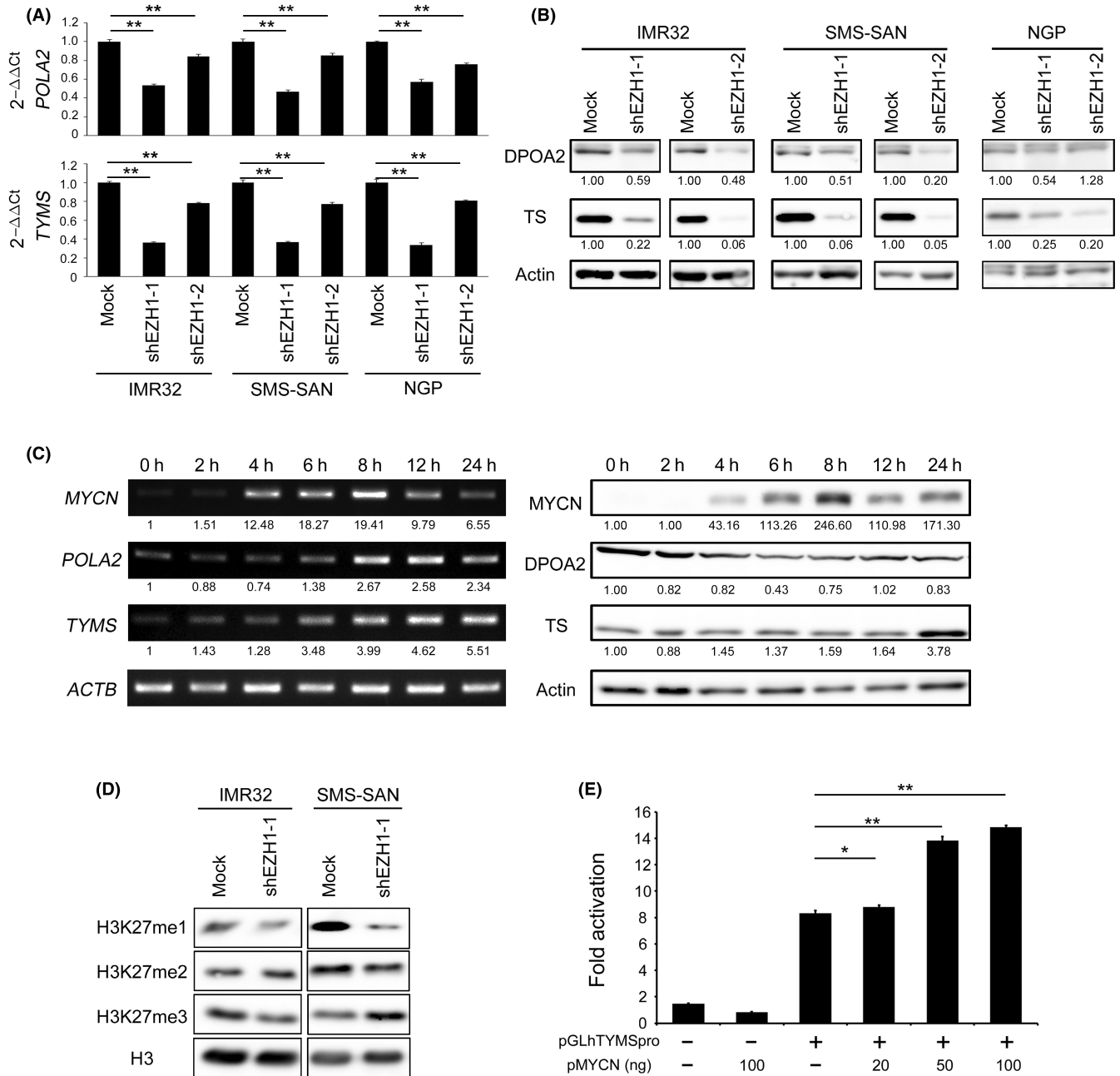
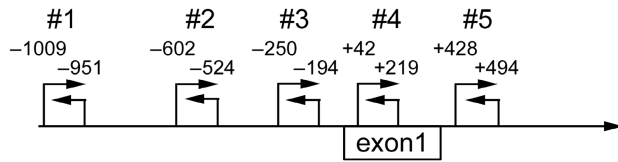


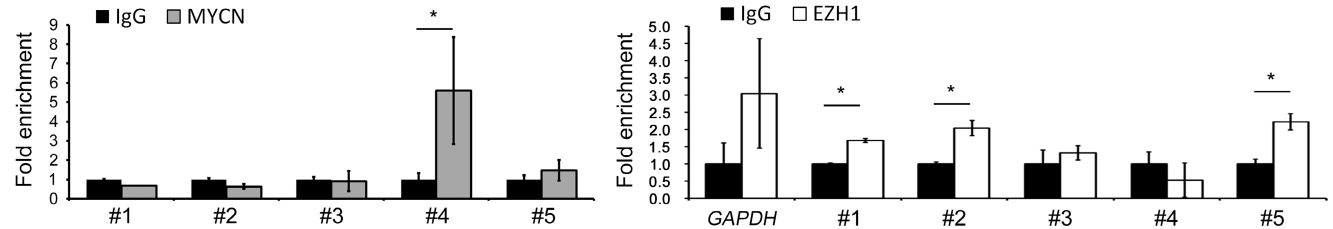
FIGURE 5 *POLA2* and *TYMS* expression is regulated by *EZH1* and *MYCN*. (A) *POLA2* and *TYMS* expression in *EZH1*-knocked down neuroblastoma cell lines analyzed by quantitative RT-PCR. (B) Protein expression of DNA polymerase alpha 2 (DPOA2) and thymidylate synthetase (TS) by western blotting. Signal intensities were quantified by ImageJ software. (C) *POLA2* and *TYMS* expression was evaluated in *MYCN*-inducible Tet-21/N cells. After withdrawal of tetracycline from the culture medium, the cells were collected at the indicated time points and analyzed by semiquantitative RT-PCR and western blotting. Signal intensities were quantified by ImageJ software. (D) The methylation status of H3K27 was analyzed by western blotting in IMR32 and SMS-SAN cells with *EZH1* knocked down by sh*EZH1*-1. (E) Luciferase reporter assay using the *TYMS* promoter region in 293T cells. The promoter activity was compared by treatment with *MYCN*. p*MYCN*, pcDNA3-*MYCN*; pGLhTYMSpro, pGL4.17-hTYMS (-649, +324); pGLhTYMSpro+, 100ng.

FIGURE 6 *MYCN* binding to the *TYMS* promoter is regulated by *EZH1*. (A) Primer design of the *TYMS* promoter region for the quantitative ChIP assay. (B,C) Quantitative ChIP assay with anti-*MYCN* or anti-*EZH1* Ab carried out on the *TYMS* promoter region in IMR32 (B) and NB-39-nu (C) cells. Data are presented as the mean \pm SD from at least three independent experiments. $*p < 0.05$. Analysis of *GAPDH* promoter region binding of IgG or anti-*EZH1* Ab was also carried out. (D) Quantitative ChIP assay with anti-*MYCN* Ab undertaken on the *TYMS* promoter region in mock- and *EZH1*-knocked down IMR32 cells. Data are presented as the mean \pm SD from at least three independent experiments. $*p < 0.05$. (E) ChIP sequencing binding profiles on the *TYMS* promoter region for *MYCN*, H3K4me3, H3K27ac, *EZH1*, *EZH2*, and H3K27me1 in IMR32 cells. The bottom figure indicates the position of the primers for the quantitative ChIP assay.

(A) *TYMS*

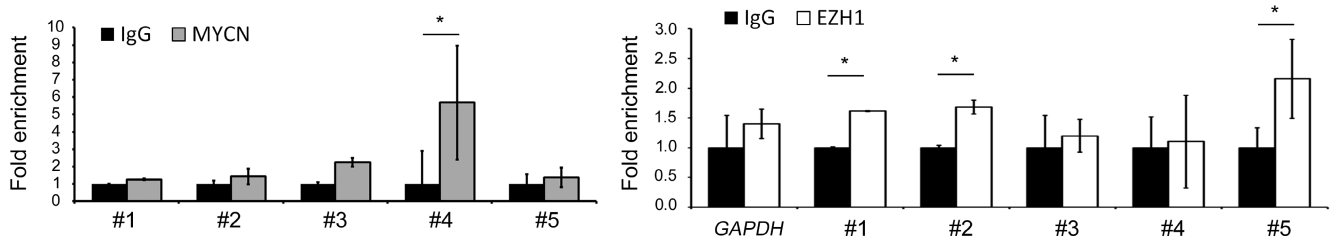
(B)

IMR32



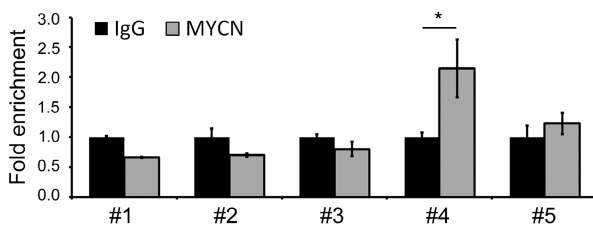
(C)

NB-39-nu

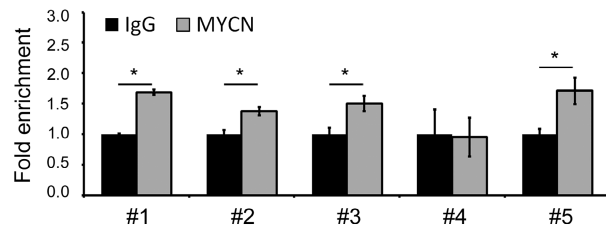


(D)

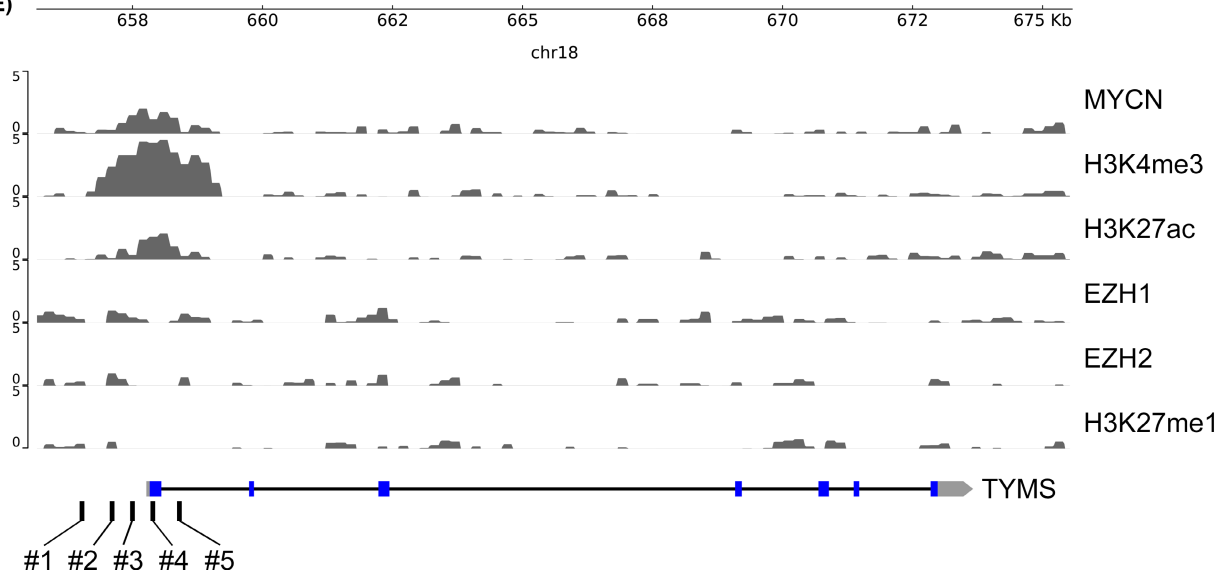
IMR32 mock



IMR32 shEZH1



(E)



epigenetic and nonepigenetic targets, being competitive with the cofactor SAM, and noncompetitive with the peptide substrate.²³ We treated the MYCN-amplified NB cells with UNC1999 because

there is no EZH1-specific inhibitor; moreover, shEZH1-1 binds to the conserved SET domain and marginally decreased the EZH2 level in NB cells (Figures S4 and S5). UNC1999 effectively decreased the

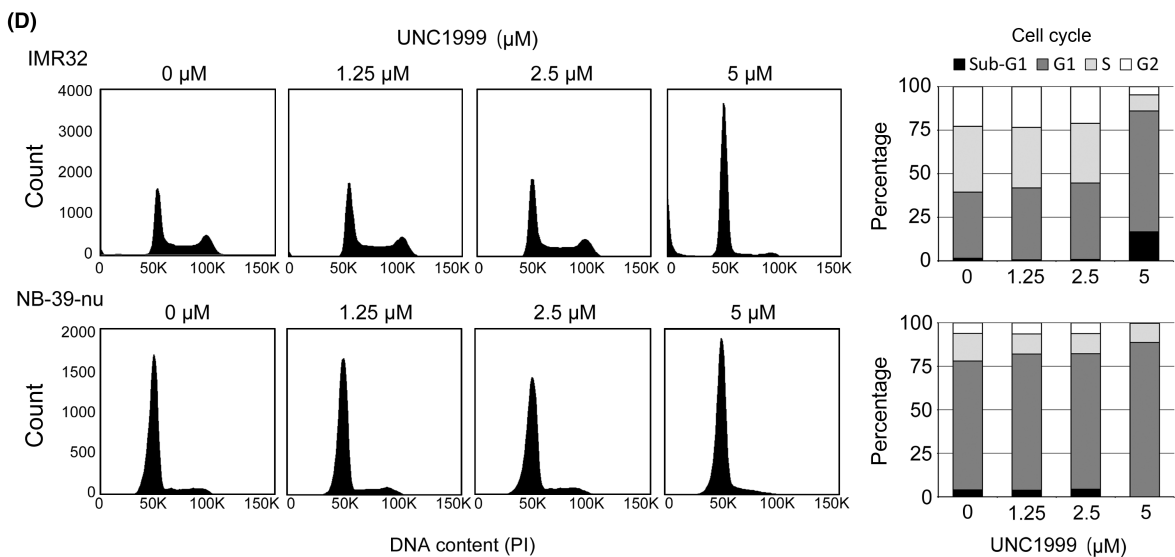
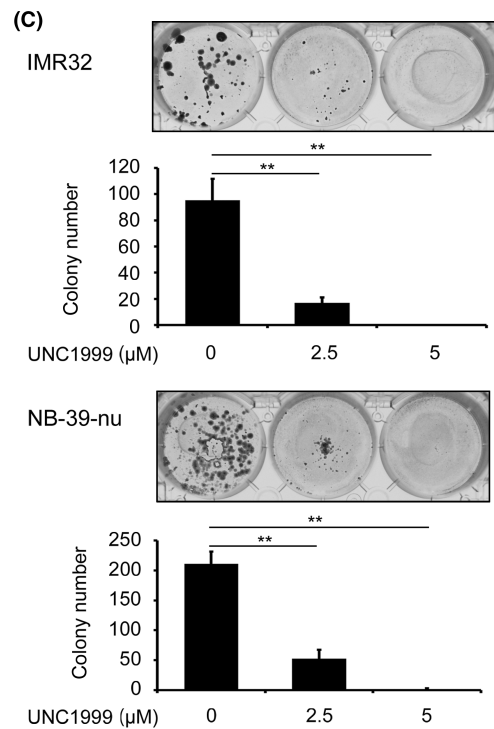
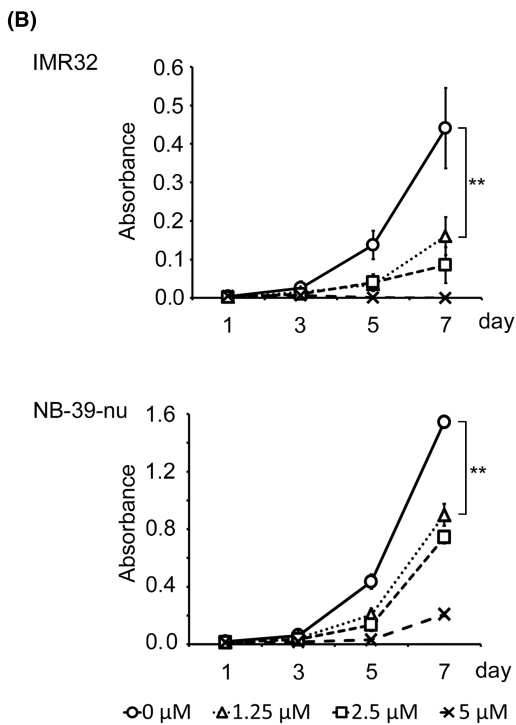
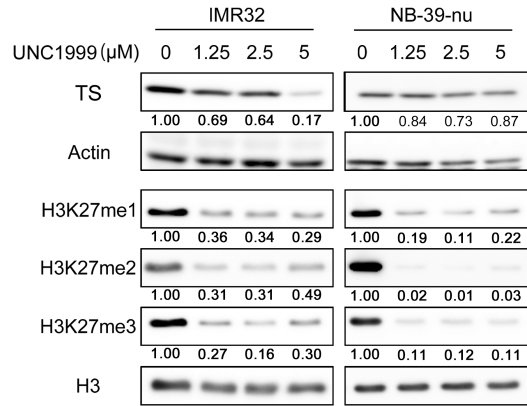
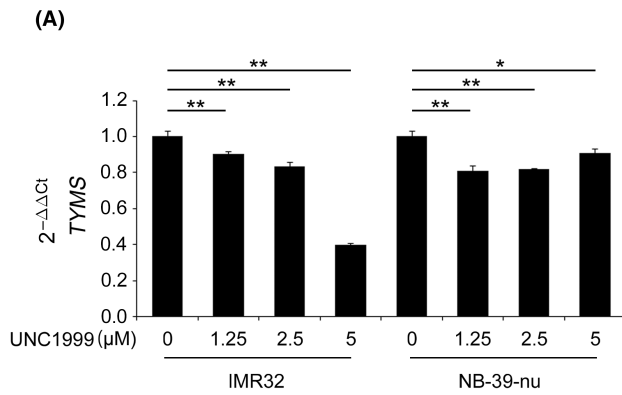


FIGURE 7 EZH1/2 inhibitor UNC1999 reduces *TYMS* expression and suppresses cell proliferation in neuroblastoma (NB) cells. (A) *TYMS* expression and H3K27 methylation status analyzed by quantitative RT-PCR and/or western blotting 48 h after UNC1999 treatment in IMR32 and NB-39-nu cells. Signal intensities were quantified by ImageJ software. (B–D) WST assay (B), colony formation assay (C), and cell cycle analysis by flow cytometry (D) of UNC1999-treated NB cells. Data are presented as the mean \pm SD from at least three independent experiments (B,C). * $p < 0.05$, ** $p < 0.01$.

H3K27me1-3 level in NB cells and reduced *TYMS* mRNA expression levels at 5 μ M (Figure 7A). Neuroblastoma cell proliferation was significantly suppressed by 1.25 μ M UNC1999 (Figure 7B,C) and the sub- G_0/G_1 apoptotic fraction was increased with 5 μ M UNC1999 treatment (Figure 7D).

3.7 | EZH inhibitor UNC1999 and 5-FU synergistically inhibit NB cell proliferation

For the chemotherapeutic treatment of NB, 5-FU does not show good efficacy due to the acquisition of resistance, as evidenced by several in vitro studies of 5-FU treatment to NB cells.^{24,25} The target enzyme for 5-FU is TS, encoded by *TYMS*. Indeed, TS expression predicts the response to 5-FU-based chemotherapy, and the expression seems to be determined by the *TYMS* promoter.²⁶ Therefore, we studied the effects of UNC1999 on 5-FU-treated NB cells. The IC_{50} value of 5-FU was 2.34 μ M in IMR32 cells and 4.68 μ M in NB-39-nu cells (Figure S6). Accordingly, we treated NB cells with 5-FU and/or UNC1999 at these concentrations. The WST-8 assay (Figure 8A) and colony formation assay (Figure 8B) showed that UNC1999 significantly enhanced the suppression of proliferation by 5-FU. We also observed a synergistic anti-NB cell proliferation effect of UNC1999 and 5-FU in NB-39-nu cells (Figure 8C; combination indexes were less than 1.0 at several points). Furthermore, the combined treatment with UNC1999 and 5-FU in xenograft experiments also significantly suppressed tumor growth (Figure 8D,E) and the necrotic area was enlarged in combination-treated NB cells (Figure 8F). The combined treatment also decreased H3K27me1-3 signals, and TS signals were increased (Figure S7). Together, because DNA methylation was not observed in the *TYMS* promoter region of NB tumors (Figure S8), our findings indicate that EZH inhibition appears to sensitize *MYCN*-amplified NB cells to 5-FU by epigenetic modification of H3K27 methylation of the *TYMS* promoter region.

4 | DISCUSSION

For development of new epigenetic therapies of advanced NB tumors, we considered that inactivation of EZH2 and its homolog EZH1 could be effective, and evaluated this possibility in the present study by undertaking EZH1 depletion in NB cell lines. Unexpectedly, only EZH1 depletion induced significant cell death in several NB cell lines. Transcriptome analysis of EZH1-depleted NB cells indicated the downregulation of several cell cycle progression-related pathways. The three cell cycle-related genes *TYMS*, *POLA2*, and

CCNA1, overlapped among the genes that were downregulated by EZH1 knockdown. Importantly, our previous transcriptome analysis in EZH2-knocked down NB cells did not indicate downregulation of *TYMS*, *POLA2*, and *CCNA1* expression.¹⁰ We further focused on *TYMS* because this gene encodes the enzyme responsible for catalyzing 5-FU and is thus related to the acquisition of 5-FU resistance acting as an oncogene in tumor cells.²⁷ EZH1 knockdown strikingly suppressed *TYMS* (protein: TS) expression at both the mRNA and protein levels in NB cells. EZH1/2 inhibition by UNC1999 also suppressed *TYMS* mRNA and protein expression and decreased all H3K27me1-3 signals. Of note, the EZH2 inhibitor EPZ6438 did not significantly suppress *TYMS* expression in several NB cell lines (FC < 1.0, Yuki Endo, 2020, unpublished data), further suggesting that EZH1 inhibition suppresses *TYMS* transcription. Furthermore, our cell proliferation assays indicated the synergistic effects of the EZH inhibitor UNC1999 with 5-FU. In our EZH1 knockdown experiments, only the H3K27me1 signal was decreased, although the EZH1/2 inhibitor UNC1999 is known to suppress the H3K27me1-3 signals. Of note, the effects of EZH1 knockdown on induction of cell death was more obvious than the effects of UNC1999, suggesting the following possibilities: (i) the balance of H3K27 methylation could be important for NB cell death, and (ii) EZH1 protein itself might have roles in preventing cell death besides its histone methylase activities. In *Eed*-KO mouse cells, both H3K27me3 and H3K27me1 signals were profoundly decreased, although the H3K4me2 signal was not, whereas in *Ezh2*-KO mouse cells, only the H3K27me3 signal was decreased.²⁸ This indicated that not only the canonical EZH2-PRC2 complex, but also the noncanonical EZH1-PRC2 complex will be important for H3K27 methylation signals. In the present study, immunoprecipitation experiments suggested the existence of an EZH1-MYCN complex. Thus, further study of the functional and physical interaction of MYCN and PRC2 proteins will be required to clarify the molecular mechanism of EZH1/2 inhibition-induced NB cell arrest and cell death.

A confounding feature of the mammalian PRC2 complexes is the existence of two highly conserved enzymatic subunits, EZH1 and EZH2, with nearly identical catalytic SET domains.²⁹ Although the role of EZH2 in H3K27me3-mediated transcriptional repression has been well established,³⁰⁻³³ the function of EZH1-PRC2 remains elusive and controversial; EZH1 complements EZH2 to maintain repressive chromatin and stem cell identity in embryonic and tissue stem cells.³⁻⁵ Of note, *Ezh1* predominantly targets H3K4me3-marked active promoters and promotes RNA polymerase (Pol) II elongation in the hippocampal neurons and differentiating muscle cells.⁷⁻⁹ In the present study, *TYMS* was identified as a MYCN-target gene, and EZH1 cooperation for transcription was observed by biochemical and qChIP and ChIPseq experiments. EZH1/2 and H3K27me1

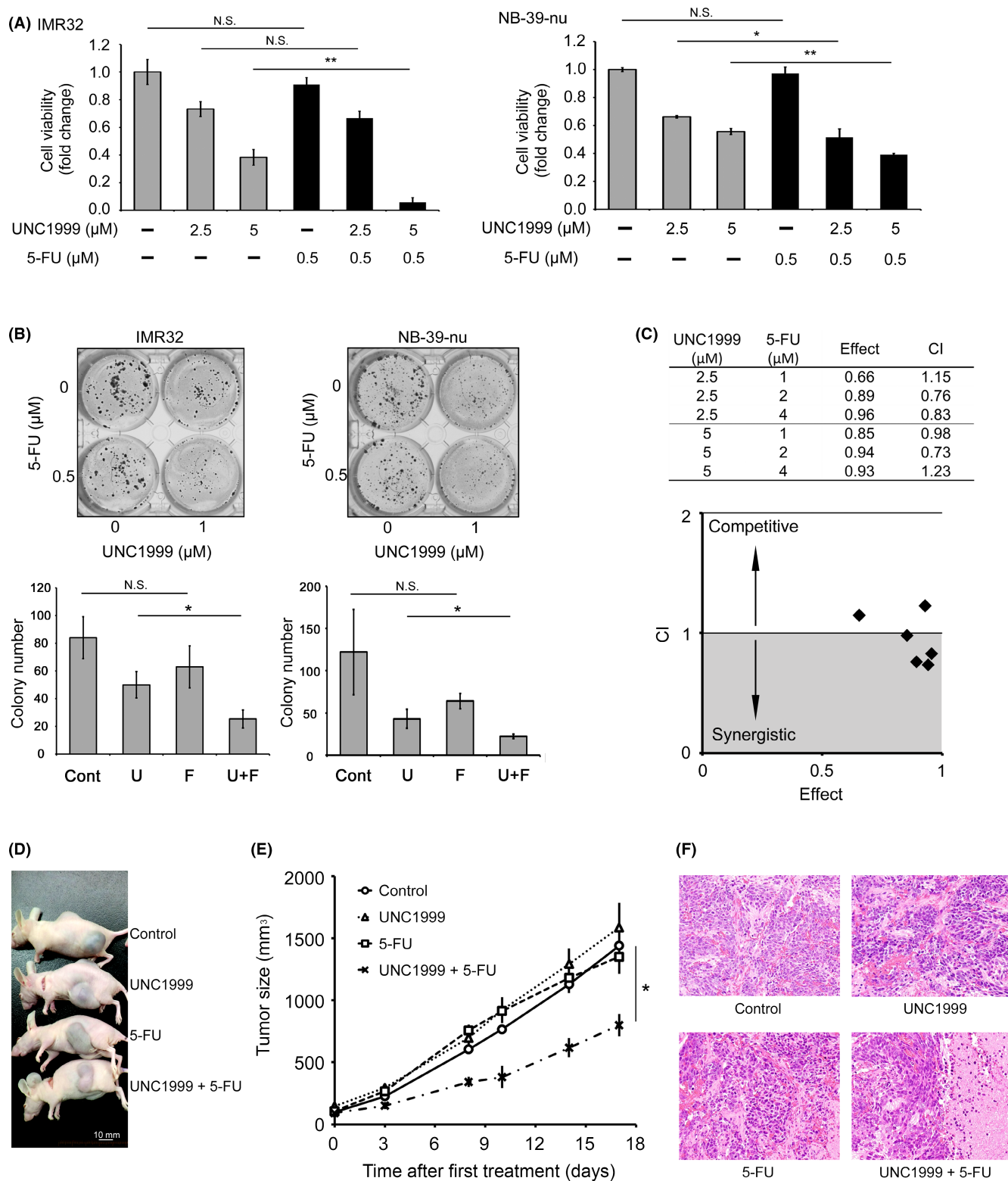


FIGURE 8 Combined treatment with UNC1999 and 5-fluorouracil (5-FU) suppresses neuroblastoma cells synergistically. (A,B) In vitro cell proliferation assay of UNC1999 and 5-FU combination therapy. WST assay (A) and colony formation assay (B) of IMR32 and NB-39-nu cells. In the WST assay, cell viability was expressed as the fold change of absorbance relative to the control value (no treatment sample) 3 days after treatment. In the colony formation assay, colonies were counted at 10 days after treatment. Data are presented as the mean \pm SD from at least three independent experiments. * $p < 0.05$, ** $p < 0.01$. Cont, control; F, 5-FU; N.S., not significant; U, UNC1999. (C) Combination index (CI) was calculated in the WST assay of NGP cells treated with several doses of UNC1999 and 5-FU. $CI < 1$ means a synergistic effect of the combination. (D,E) Tumor developments in BALB/cAJcl nu/nu mice following the injection of IMR32 cells were measured. They were treated with mock, UNC1999, 5-FU, and combination. Data are presented as the mean \pm SD of tumors in four mice. * $p < 0.05$. (F) H&E staining of xenograft tumors treated with mock, UNC1999, 5-FU, and combination.

ChIPseq indicated that EZH1/2 binding was not significantly colocalized with H3K27me1 marks not only in the genome-wide analysis, but also in the TYMS locus (Figures 6E and S9). However, H3K27methylase inhibitor UNC1999 inhibited TYMS transcription (Figure 7), suggesting the complicated effects of EZH1 inhibition on MYCN-related transcriptional regulation.

This is the first report showing that EZH inhibition affects the transcription of genes related to tumor cell proliferation and chemotherapeutic drug resistance in NB cells. These findings will be informative for the development of epigenetic therapies and new chemotherapy protocols for patients with MYCN-amplified NB with an unfavorable prognosis.

AUTHOR CONTRIBUTIONS

Conceptualization: TK, TH, HY. Data curation: YS, HT, YE, RO, MH, DS, SS, JA, KM, TW, MO. Formal analysis: YS, HT, SS, AN, MH, KC, KM, MO, TK. Funding acquisition: MO, TH, TK. Project administration: TK. Resources: TK. Software: RS. Analyzed data: YS, HT, RS, MO, TK. Supervision: TK. Validation: YS, HT, AN, MO, TK. Visualization: YS, HT, AN, MO, TK. Writing original draft: YS, HT, TH, TK. Writing review and editing: TK.

ACKNOWLEDGMENTS

We thank Ms. N. Kawanabe, Ms. K. Tachikawa, and Ms. H. Odagawa for their technical assistance, and Editage for English language editing. Financial support for this study was provided by Saitama Cancer Center. This study was partly supported by JSPS KAKENHI Grant Number JP19K18022 and a JSPS KAKENHI Grant-in-Aid for Scientific Research (B) Number JP19H03625.

FUNDING INFORMATION

Saitama Cancer Center; Japan Society for the Promotion of Science (JSPS) KAKENHI, Grant/Award Number: JP19K18022; JSPS KAKENHI Grant-in-Aid for Scientific Research (B), Grant/Award Number: JP19H03625.

DISCLOSURE

Takehiko Kamijo and Miki Ohira are Editors of *Cancer Science*. The other authors have no conflict of interest.

DATA AVAILABILITY STATEMENT

The datasets supporting the conclusions of this article are available from the NCBI's GEO and are accessible through GEO accession numbers GSE162057 and GSE188673. The ChIPseq data of EZH1 and H3K27me1 are being prepared for registration.

ETHICS STATEMENT











Approval of the research protocol by an Institutional Review Board: This study was approved by the ethics committee of the Saitama Cancer Center (approval number 759).

Informed consent: Written informed consent was obtained from all patients.

Registry and registration no. of the study/trial.: N/A.

Animal studies: All animals were maintained and used for experiments in accordance with the guidelines of the Institutional Animal Experiments Committee of Saitama Cancer Center.

ORCID

Hisanori Takenobu  <https://orcid.org/0000-0001-7355-1565>
 Yuki Endo  <https://orcid.org/0000-0002-5658-0142>
 Kyosuke Mukae  <https://orcid.org/0000-0001-6411-2990>
 Dilibaerguli Shaliman  <https://orcid.org/0000-0003-2421-5690>
 Jesmin Akter  <https://orcid.org/0000-0002-4573-1603>
 Kiyohiro Ando  <https://orcid.org/0000-0002-2876-3304>
 Atsuko Nakazawa  <https://orcid.org/0000-0002-9008-4281>
 Miki Ohira  <https://orcid.org/0000-0001-9105-1142>
 Tomoro Hishiki  <https://orcid.org/0000-0002-2515-1054>
 Takehiko Kamijo  <https://orcid.org/0000-0003-4798-7546>

REFERENCES

- Schuettengruber B, Bourbon HM, Di Croce L, Cavalli G. Genome regulation by Polycomb and Trithorax: 70 years and counting. *Cell*. 2017;171:34-57. doi:10.1016/j.cell.2017.08.002
- Blackledge NP, Rose NR, Klose RJ. Targeting Polycomb systems to regulate gene expression: modifications to a complex story. *Nat Rev Mol Cell Biol*. 2015;16:643-649. doi:10.1038/nrm4067
- Ezhkova E, Lien WH, Stokes N, Pasolli HA, Silva JM, Fuchs E. EZH1 and EZH2 cogovern histone H3K27 trimethylation and are essential for hair follicle homeostasis and wound repair. *Genes Dev*. 2011;25:485-498. doi:10.1101/gad.2019811
- Margueron R, Li G, Sarma K, et al. Ezh1 and Ezh2 maintain repressive chromatin through different mechanisms. *Mol Cell*. 2008;32:503-518. doi:10.1016/j.molcel.2008.11.004
- Shen X, Liu Y, Hsu YJ, et al. EZH1 mediates methylation on histone H3 lysine 27 and complements EZH2 in maintaining stem cell identity and executing pluripotency. *Mol Cell*. 2008;32:491-502. doi:10.1016/j.molcel.2008.10.016
- Ho L, Crabtree GR. An EZ mark to miss. *Cell Stem Cell*. 2008;3:577-578. doi:10.1016/j.stem.2008.11.007
- Henriquez B, Bustos FJ, Aguilar R, et al. Ezh1 and Ezh2 differentially regulate PSD-95 gene transcription in developing hippocampal neurons. *Mol Cell Neurosci*. 2013;57:130-143. doi:10.1016/j.mcn.2013.07.012
- Mousavi K, Zare H, Wang AH, Sartorelli V. Polycomb protein Ezh1 promotes RNA polymerase II elongation. *Mol Cell*. 2012;45:255-262. doi:10.1016/j.molcel.2011.11.019
- Stojic L, Jasencakova Z, Prezioso C, et al. Chromatin regulated interchange between polycomb repressive complex 2 (PRC2)-Ezh2 and PRC2-Ezh1 complexes controls myogenin activation in skeletal muscle cells. *Epigenetics Chromatin*. 2011;4:16. doi:10.1186/1756-8935-4-16
- Li Z, Takenobu H, Setyawati AN, et al. EZH2 regulates neuroblastoma cell differentiation via NTRK1 promoter epigenetic modifications. *Oncogene*. 2018;37:2714-2727. doi:10.1038/s41388-018-0133-3
- Lutz W, Stöhr M, Schürmann J, Wenzel A, Löhr A, Schwab M. Conditional expression of N-myc in human neuroblastoma cells increases expression of alpha-prothymosin and ornithine decarboxylase and accelerates progression into S-phase early after mitogenic stimulation of quiescent cells. *Oncogene*. 1996;13:803-812.
- Tsubota S, Kishida S, Shimamura T, et al. PRC2-mediated transcriptional alterations at the embryonic stage govern tumorigenesis

- and clinical outcome in MYCN-driven neuroblastoma. *Cancer Res.* 2017;77:5259-5271. doi:10.1158/0008-5472.CAN-16-3144
13. Corvetta D, Chayka O, Gherardi S, et al. Physical interaction between MYCN oncogene and polycomb repressive complex 2 (PRC2) in neuroblastoma: functional and therapeutic implications. *J Biol Chem.* 2013;288:8332-8341. doi:10.1074/jbc.M113.454280
 14. Xu J, Shao Z, Li D, et al. Developmental control of polycomb subunit composition by GATA factors mediates a switch to non-canonical functions. *Mol Cell.* 2015;57:304-316. doi:10.1016/j.molcel.2014.12.009
 15. Vo LT, Kinney MA, Liu X, et al. Regulation of embryonic haematopoietic multipotency by EZH1. *Nature.* 2018;553:506-510. doi:10.1038/nature25435
 16. Ferrari KJ, Scelfo A, Jammula S, et al. Polycomb-dependent H3K27me1 and H3K27me2 regulate active transcription and enhancer fidelity. *Mol Cell.* 2014;53:49-62. doi:10.1016/j.molcel.2013.10.030
 17. De Preter K, Vandesompele J, Heimann P, et al. Human fetal neuroblast and neuroblastoma transcriptome analysis confirms neuroblast origin and highlights neuroblastoma candidate genes. *Genome Biol.* 2006;7:R84. doi:10.1186/gb-2006-7-9-r84
 18. Morozova O, Vojvodic M, Grinshtein N, et al. System-level analysis of neuroblastoma tumor-initiating cells implicates AURKB as a novel drug target for neuroblastoma. *Clin Cancer Res.* 2010;16:4572-4582. doi:10.1158/1078-0432.CCR-10-0627
 19. Gogolin S, Batra R, Harder N, et al. MYCN-mediated overexpression of mitotic spindle regulatory genes and loss of p53-p21 function jointly support the survival of tetraploid neuroblastoma cells. *Cancer Lett.* 2013;331:35-45. doi:10.1016/j.canlet.2012.11.028
 20. Valentijn LJ, Koster J, Haneveld F, et al. Functional MYCN signature predicts outcome of neuroblastoma irrespective of MYCN amplification. *Proc Natl Acad Sci U S A.* 2012;109:19190-19195. doi:10.1073/pnas.1208215109
 21. Fang WH, Wang Q, Li HM, Ahmed M, Kumar P, Kumar S. PAX3 in neuroblastoma: oncogenic potential, chemosensitivity and signalling pathways. *J Cell Mol Med.* 2014;18:38-48. doi:10.1111/jcmm.12155
 22. Mannava S, Grachtchouk V, Wheeler LJ, et al. Direct role of nucleotide metabolism in C-MYC-dependent proliferation of melanoma cells. *Cell Cycle.* 2008;7:2392-2400. doi:10.4161/cc.6390
 23. Konze KD, Ma A, Li F, et al. An orally bioavailable chemical probe of the lysine methyltransferases EZH2 and EZH1. *ACS Chem Biol.* 2013;8:1324-1334. doi:10.1021/cb400133j
 24. Fulda S, Honer M, Menke-Moellers I, Berthold F. Antiproliferative potential of cytostatic drugs on neuroblastoma cells in vitro. *Eur J Cancer.* 1995;31A:616-621. doi:10.1016/0959-8049(95)00055-N
 25. Makino S, Kashii A, Kanazawa K, Tsuchida Y. Effects of newly introduced chemotherapeutic agents on a cytogenetically highly malignant neuroblastoma, xenotransplanted in nude mice. *J Pediatr Surg.* 1993;28:612-616.
 26. Lecomte T, Ferraz JM, Zinzindohoué F, et al. Thymidylate synthase gene polymorphism predicts toxicity in colorectal cancer patients receiving 5-fluorouracil-based chemotherapy. *Clin Cancer Res.* 2004;10:5880-5888. doi:10.1158/1078-0432.CCR-04-0169
 27. Rahman L, Voeller D, Rahman M, et al. Thymidylate synthase as an oncogene: a novel role for an essential DNA synthesis enzyme. *Cancer Cell.* 2004;5:341-351. doi:10.1016/S1535-6108(04)00080-7
 28. Xie H, Xu J, Hsu JH, et al. Polycomb repressive complex 2 regulates normal hematopoietic stem cell function in a developmental-stage-specific manner. *Cell Stem Cell.* 2014;14:68-80. doi:10.1016/j.stem.2013.10.001
 29. Laible G, Wolf A, Dorn R, et al. Mammalian homologues of the Polycomb-group gene enhancer of zeste mediate gene silencing in drosophila heterochromatin and at *S. cerevisiae* telomeres. *EMBO J.* 1997;16:3219-3232. doi:10.1093/emboj/16.11.3219
 30. Cao R, Wang L, Wang H, et al. Role of histone H3 lysine 27 methylation in Polycomb-group silencing. *Science.* 2002;298:1039-1043. doi:10.1126/science.1076997
 31. Czermin B, Melfi R, McCabe D, Seitz V, Imhof A, Pirrotta V. *Drosophila* enhancer of Zeste/ESC complexes have a histone H3 methyltransferase activity that marks chromosomal Polycomb sites. *Cell.* 2002;111:185-196. doi:10.1016/S0092-8674(02)00975-3
 32. Kuzmichev A, Nishioka K, Erdjument-Bromage H, Tempst P, Reinberg D. Histone methyltransferase activity associated with a human multiprotein complex containing the enhancer of Zeste protein. *Genes Dev.* 2002;16:2893-2905. doi:10.1101/gad.1035902
 33. Müller J, Hart CM, Francis NJ, et al. Histone methyltransferase activity of a *drosophila* Polycomb group repressor complex. *Cell.* 2002;111:197-208. doi:10.1016/S0092-8674(02)00976-5

SUPPORTING INFORMATION

Additional supporting information can be found online in the Supporting Information section at the end of this article.

How to cite this article: Shinno Y, Takenobu H, Sugino RP, et al. Polycomb EZH1 regulates cell cycle/5-fluorouracil sensitivity of neuroblastoma cells in concert with MYCN. *Cancer Sci.* 2022;113:4193-4206. doi: [10.1111/cas.15555](https://doi.org/10.1111/cas.15555)